JACS JOURNAL OF THE AMERICAN CHEMICAL SOCIETY

Article

Cite This: J. Am. Chem. Soc. 2018, 140, 13503−13513

pubs.acs.org/JACS

Halogen Bond Asymmetry in Solution

Sofia Lindblad,[†,‡] Krenare Mehmeti,[†] Alberte X. Veiga,[†,∥] Bijan Nekoueishahraki,[†] Jürgen Gräfenstein,[†] and Máté Erdélyi*[,†,§,‡]

[†]Department of Chemistry and Molecular Biology, University of Gothenburg, SE-412 96 Gothenburg, Sweden

[‡]Department of Chemistry − BMC, Uppsala University, SE-751 23 Uppsala, Sweden

[§]The Swedish NMR Centre, Medicinaregatan 5C, SE-413 90 Gothenburg, Sweden

Supporting Information

ABSTRACT: Halogen bonding is the noncovalent interaction of halogen atoms in which they act as electron acceptors. Whereas three-center hydrogen bond complexes, $[D\cdots H\cdots D]^+$ where D is an electron donor, exist in solution as rapidly equilibrating asymmetric species, the analogous halogen bonds, $[D\cdots X\cdots D]^+$, have been observed so far only to adopt static and symmetric geometries. Herein, we investigate whether halogen bond asymmetry, i.e., a $[D{-}X\cdots D]^+$ bond geometry, in which one of the D−X bonds is shorter and stronger, could be induced by modulation of electronic or steric factors. We have also attempted to convert a static three-center halogen bond complex into a mixture of rapidly exchanging asymmetric isomers, $[D\cdots X{-}D]^+ \rightleftarrows [D{-}X\cdots D]^+$, corresponding to the preferred form of the analogous hydrogen bonded complexes. Using ^{15}N NMR, IPE NMR, and DFT, we prove that a static, asymmetric geometry, $[D{-}X\cdots D]^+$, is obtained upon desymmetrization of the electron density of a complex. We demonstrate computationally that conversion into a dynamic mixture of asymmetric geometries, $[D\cdots X{-}D]^+ \rightleftarrows [D{-}X\cdots D]^+$, is achievable upon increasing the donor−donor distance. However, due to the high energetic gain upon formation of the three-center-four-electron halogen bond, the assessed complex strongly prefers to form a dimer with two static and symmetric three-center halogen bonds over a dynamic and asymmetric halogen bonded form. Our observations indicate a vastly different preference in the secondary bonding of H^+ and X^+. Understanding the consequences of electronic and steric influences on the strength and geometry of the three-center halogen bond provides useful knowledge on chemical bonding and for the development of improved halonium transfer agents.

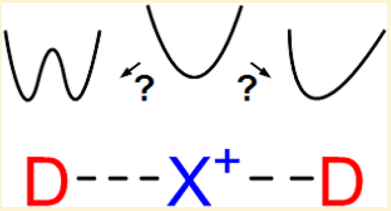

INTRODUCTION

Halogen bonding (XB) is the attractive, noncovalent interaction of an electron-poor region of a halogen with a Lewis base.[1,2] It resembles hydrogen bonding in strength and directionality, yet has different geometrical requirements due to the larger van der Waals radii of halogen atoms (r_wI = 1.98 Å, r_wBr = 1.85 Å, r_wCl = 1.75 Å, r_wF = 1.47 Å, whereas r_wH = 1.2 Å).[3] Although it has already been observed one and a half centuries ago,[4−6] the halogen bond phenomenon has for long been neglected and remains considerably unexplored. However, recent X-ray crystallographic work[2] has inspired a resurgence of interest and rationalizations based on the σ-hole[7] and charge transfer concepts.[8] Halogen bonding has led to numerous applications, including crystal engineering,[9] material sciences,[10] structural biology,[11] medicinal[12] and solution[13] chemistries, as well as in organocatalysis.[14]

Following early investigations,[4,5,15−18] a major leap enabling the systematic experimental assessment of halogen bonding was the introduction of perfluorinated halogen bond donors by Resnati and co-workers.[19] These promote the formation of a large electrophilic area on a halogen, i.e. a σ-hole, and consequently strong and thereby easy to detect halogen bonds.[20,21] An alternative approach, introduced by us, is to increase bond strength by the use of a positively charged halogen, formally a halonium ion or halogen(I), X^+, as halogen bond donor.[6,22,23] In such complexes, X^+ forms a halogen bond with two Lewis bases simultaneously, each contributing with a lone pair of electrons.[23,24] Studies on the nature of the X^+-centered halogen bonds[25,26] and the possible influence of solvent,[27] counterion,[28] electron density,[29] and the identity of the halogen[26] on its geometry, demonstrated that the heavy halogens form static, symmetric three-center arrangements, $[D\cdots X\cdots D]^+$, where D is an electron donor. This geometry possesses remarkably short (R_{XB} = 0.65−0.69)[26,30] and strong (up to 120 kJ/mol)[13,25] halogen bonds and is formed with nitrogenous,[23,31] sulphurous,[32,33] selenious, and tellurious[34] halogen bond acceptors. Owing to its extraordinary strength, the three-center halogen bond can be used for stabilization of large supramolecular assemblies.[35,36] Moreover, such complexes are synthetically applicable as halonium transfer and oxidation agents.[29,37−51] We have shown that the three-center halogen bond has a partial covalent character that increases with the decrease in size of the halogen(I),[25,26] an observation recently confirmed by Fourmigué et al.[52] Halogen bond strength, however, increases with the size of the halogen and thus with the increase in ionic character (and the decrease in covalent character) of the bond.[26]

Received: September 1, 2018
Published: September 20, 2018

DOI: 10.1021/jacs.8b09467
J. Am. Chem. Soc. 2018, 140, 13503−13513

The geometry of a three-centered halogen bond may be static and centrosymmetric, $[D\cdots X\cdots D]^+$, with the central halogen(I) possessing two equally strong and equally long halogen bonds. The motion of the halogen in such systems is described by a single-well energy potential (Figure 1a).

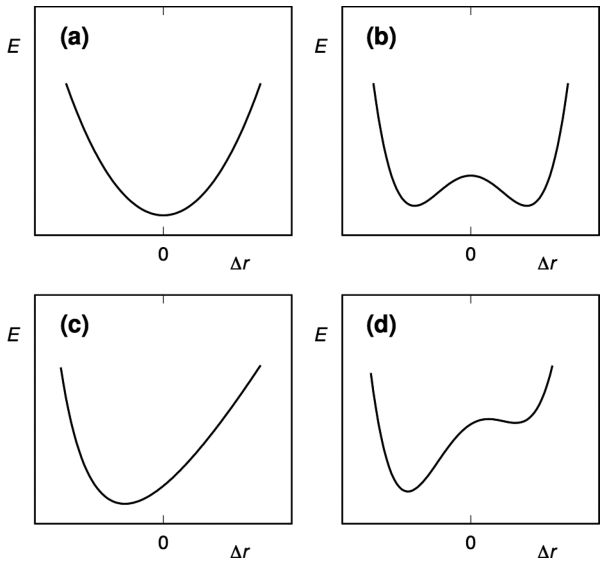

Figure 1. Energy potentials of halogen motion in a three-center $[D\cdots X\cdots D]^+$ halogen bond: (a) a symmetric single-well energy potential describes the halogen motion when the D−X bonds are equal and the system is static and symmetric, whereas (b) a symmetric double-well potential may reflect a pair of asymmetric isomers, $[D\cdots X{-}D]^+ \rightleftarrows [D{-}X\cdots D]^+$, in dynamic equilibrium, with each form having a shorter and stronger D−X and a longer and weaker D···X bond when the energy barrier between the minima is shallow. The system becomes static and asymmetric if the energy barrier between the two minima is high. Alternatively, if the electron density of the two Lewis bases, D, are different, the halogen motion may either follow (c) an asymmetric single-well potential, or (d) an asymmetric double-well potential with a clear preference for a shorter and stronger bond toward one of the electron donors. The potential energy variation is shown here as a function of Δr, the displacement of X^+ from the symmetrical position.

Alternatively, the geometry may be asymmetric, $[D{-}X\cdots D]^+$, with one stronger and shorter, D−X, bond to one of the electron donors, and a weaker and longer, D···X, bond to the other donor (Figure 1b). The D−X bond of this arrangement is expected to have an increased, whereas the D···X a decreased, covalent character, as compared to the bonds of the centrosymmetric $[D\cdots X\cdots D]^+$ geometry. If the Lewis basicities of the two electron donors are comparable and the two asymmetric geometries, $[D{-}X\cdots D]^+$ and $[D\cdots X{-}D]^+$, are separated by a shallow energy barrier, these may interconvert, and the system will exist as a dynamic mixture in which the halogen motion is described with a symmetric double-well energy potential (Figure 1b). Analogous to the term prototropy that describes tautomeric exchange processes involving the transfer of a proton, such a low barrier $[D{-}X\cdots D]^+ \rightleftarrows [D\cdots X{-}D]^+$ interconversion may be designated as halotropy. If the two geometries, $[D\cdots X{-}D]^+$ and $[D{-}X\cdots D]^+$, are separated by a high-energy barrier, the complex converts into a static, asymmetric geometry that has a conventional covalent and a conventional halogen bond, $D{-}X^+\cdots D$. The halogen of the latter has a classic σ-hole[7] and, accordingly, a covalent and secondary bond, whereas that of the three-center-four electron $[D\cdots X\cdots D]^+$ complex possesses a p-hole, formed by the empty p-orbital of X^+, as well as two secondary bonds with a partial covalent character.[23] If the electron donors have slightly different Lewis basicities, the complex may either become (Figure 1c) static and asymmetric, with the halogen showing a higher preference to one of the Lewis bases and its motion between the electron donors being described by an asymmetric single-well, or it is expected to form (Figure 1d) asymmetric geometries that are of different energy. In the latter system, the halogen motion is described by an asymmetric double-well, where one of the minima is of lower energy and of higher stability (Figure 1d).

The halogen motion in a three-center halogen bond is analogous to the $[LG{-}C\cdots Nu]^+ \rightleftarrows [LG\cdots C\cdots Nu]^+ \rightleftarrows [LG\cdots C{-}Nu]^+$ process, where Nu denotes a nucleophile and LG a leaving group in the transition state of, e.g., an S_N2 reaction.[26,53,54] The energy profile of this reaction is the inverse of that of halonium transfer, with the transition state being an energy maximum. Owing to the different Lewis basicities of the nucleophile and of the leaving group, it shows highest analogy to the static asymmetric three-center halogen bond system, whose energy profile is shown in Figure 1c.

Electrophilic halogenations involve the same general halonium transfer process: (i) an initial weakening of a covalent dihalogen bond; (ii) formation of a three-center complex consisting of a nucleophile, the central halogen(I) center and a leaving group (e.g., a halide ion); (iii) collapse of this intermediate upon formation of a covalent halogen-nucleophile bond and leaving group elimination.

The $[D{-}X\cdots D]^+$, $[D\cdots X\cdots D]^+$, and $[D\cdots X{-}D]^+$ species can also be seen to represent varying stages of a halonium ion transfer process from one halogen bond acceptor to another. These stages possess a varying degree of covalency and varying D−X bond lengths. Understanding whether a halogen transfer in between two halogen bond acceptors follows a single-well or double-well potential, whether it takes place at all, and whether the symmetric transition geometry possesses higher stability than the resonance stabilized equilibrating mixture of asymmetric ones is of fundamental interest and has recently received an increasing attention.[23,52,55−57]

To date, all reported X^+-centered halogen bonds formed by the coordination of two electron donors of comparable basicity have been described as symmetric.[23,34] Neither solvent polarity,[27] ion coordination,[58] nor symmetric alteration of the electron density[29] could desymmetrize the centrosymmetric $[D\cdots X\cdots D]^+$ geometries of these systems. Asymmetric arrangements could, so far, only be achieved by using two Lewis bases with vastly different Lewis basicities.[52,57] By contrast, analogous hydrogen bond $[D{-}H{-}D]^+$ complexes prefer asymmetric geometry.[59,60] Herein, we evaluate whether the strongly favored symmetric three-center halogen bond, $[D\cdots X\cdots D]^+$, may be converted into a static and asymmetric geometry (Figure 1c), $[D{-}X\cdots D]^+$, or into a dynamic interconverting mixture of asymmetric complexes, $[D\cdots X{-}D]^+ \rightleftarrows [D{-}X\cdots D]^+$ (Figure 1b). The former ought to be achieved by asymmetrically adjusting the electron density of the Lewis basic moieties, D, by introduction of different electron-withdrawing versus donating substituents. The latter, a dynamic asymmetric molecular system, is expected to be obtained upon enforcing a longer-than-optimal donor−donor, here nitrogen−nitrogen, distance (**2a**). Based on computational analyses, we designed, synthesized and investigated compound **1a** (Figure 2) as a candidate for a static asymmetric

DOI: 10.1021/jacs.8b09467
J. Am. Chem. Soc. 2018, 140, 13503−13513

halogen bonded system (Figure 1c) and compound **2a** as a candidate for a dynamic asymmetric (Figure 1b) system.

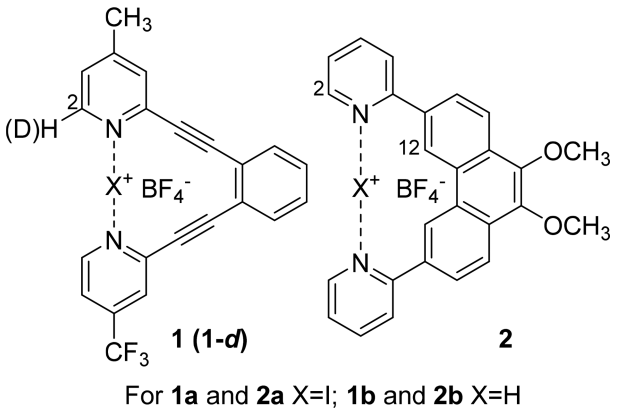

Figure 2. [(4-Methyl-2-((2-((4-(trifluoromethyl)pyridin-2-yl)-ethynyl)phenyl)ethynyl)pyridine)iodine]$^+$ tetrafluoroborate (**1**) and [(2,2′-(9,10-dimethoxyphenanthrene-3,6-diyl)dipyridine)iodine]$^+$ tetrafluoroborate (**2**) were used as model systems to study a static asymmetric and a dynamic asymmetric halogen bond, respectively. Complex **1** allows optimal N−N distance for the formation of a three-center halogen bond and has an asymmetric electron distribution. Complex **2** has a longer-than-optimal distance between its nitrogens and has a symmetric electron distribution. A mixture of **1** and its monodeuterated isotopologue **1-*d*** was used in IPE NMR experiments to differentiate between a static [N···I···N]$^+$ and a dynamic [N···I−N]$^+$ ⇄ [N−I···N]$^+$ system.

RESULTS AND DISCUSSION

Design. As a starting point for the design of asymmetrically halogen bonded systems, we studied the [N···I···N]$^+$ bond energy dependence on the nitrogen−nitrogen distance, r_{NN}, and on the displacement of the iodine(I) Δr from a symmetric geometry in [bis(pyridine)iodine]$^+$, a model system (Figure 3, computational details are given in the Supporting Information). The computed energy surface shows the global energy minimum at r_{NN} = 4.511 Å and Δr = 0, i.e., at a centrosymmetric configuration, in agreement with the literature.[22,25] Upon increasing the nitrogen−nitrogen distance, the symmetric geometry remains most stable up to r_{NN} = 4.880 Å, where a bifurcation occurs, and at larger nitrogen−nitrogen distances the asymmetric [N···I−N]$^+$ geometry becomes energetically most favorable. Upon a further increase of r_{NN}, the energy barrier between the asymmetric geometries increases, indicating them to be even more favored at large nitrogen−nitrogen distances as compared to the corresponding symmetric geometry. It should, however, be noted that these asymmetric geometries are of higher energy as compared to the symmetric geometry at the global energy minimum (r_{NN} = 4.511 Å, Δr = 0). The energy surface shown in Figure 3 does not immediately provide potential curves analogous to those shown in Figure 1, as it does not account for strain energy and for geometric constraints the backbone of **1** and **2** may impose on the [N···I···N]$^+$ bond. However, the potential curves can be qualitatively inferred from the energy surface. Hence, for a perfectly flexible ligand, the strain energy vanishes, and the potential curve shown in blue in Figure 3, and accordingly the symmetric single-well potential shown in Figure 1a, is predicted to describe the halogen's motion. A promising approach to accomplish a static asymmetric [N−I···N]$^+$ bond,

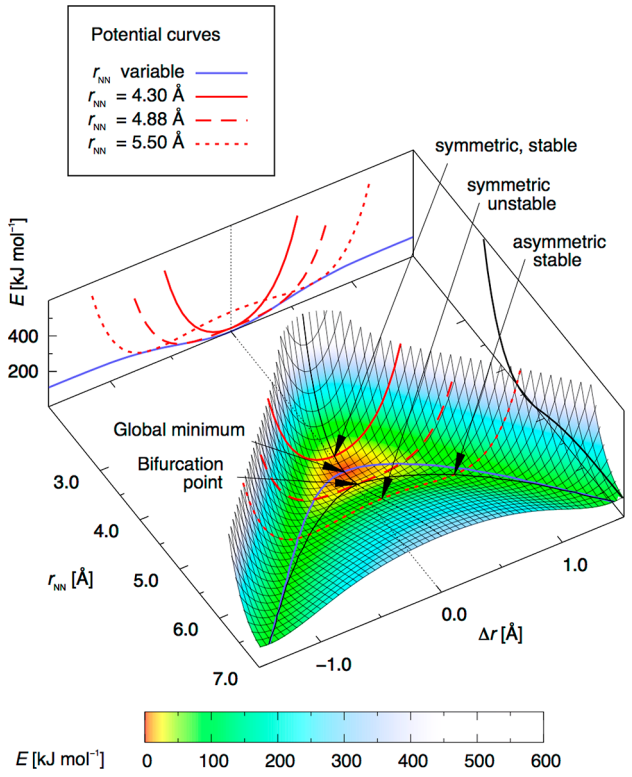

Figure 3. Variation of electronic energy as a function of the position of the iodine in an [N···I···N]$^+$ halogen bond, upon varying the N−N distance, r_{NN} (Å), and the position of the iodine as described by Δr, the elongation of the iodine from the geometrical midpoint of the nitrogen−nitrogen distance. Thus, at Δr = 0 the iodine is centered between the nitrogens, whereas at Δr = 0.5 Å it is 1 Å closer to one of them. The blue line shows the potential curve, corresponding to Figure 1a, for variable r_{NN}, while the red lines show the potential curves for r_{NN} kept fixed at 4.30 (solid), 4.88 (long-dashed), and 5.50 Å (short-dashed), respectively, shown both in the 3D plot and projected on the rear border plane. The black line on the right border plane shows the dissociation curve of the [N···I···N]$^+$ bond model system. DFT calculations were performed using the M06 exchange and correlation functional[62] and a mixed-level (double-ζ/triple-ζ/augmented triple-ζ) basis set (for details see the Supporting Information).

Figure 1c, is to add different para-substituents to the two pyridine moieties of the complex. Model calculations were performed with various combinations of para-substituted pyridine molecules, namely CH_3 and CF_3 groups, which were chosen because of their steric similarity yet highly different electronic properties, their negligible Lewis basicity, and our synthetic experience.[29] For systems with two equal substituents, the [N···I···N]$^+$ bond is stabilized (CH_3) or destabilized (CF_3), but the symmetric shape of the potential curve remains unaltered. In contrast, for the system with a CH_3 and a CF_3 substituent, an asymmetric single-well potential curve with the iodine shifted toward the CH_3-substituted pyridine by about 0.05 Å is obtained (Figure 4a, long-dashed line). In view of this, to obtain a halogen bond showing a static asymmetric single-well potential, we designed **1a**. This backbone provides a sterically symmetric but electronically asymmetric[61] environment for the central halogen of the three-center [N···I···N]$^+$ bond. For analogs of **1**, we have shown that due to the flexibility of the acetylenes, the backbone exerts only a weak strain on the [N···I···N]$^+$ halogen bond.[25] For the

DOI: 10.1021/jacs.8b09467
J. Am. Chem. Soc. 2018, 140, 13503−13513

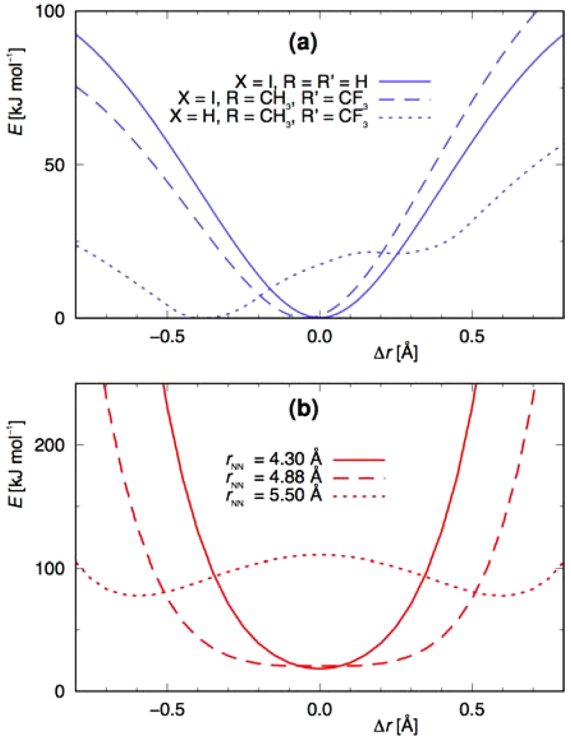

Figure 4. Potential energy curves of $[N\cdots I\cdots N]^+$ halogen bonds: (a) Potential curves of complexes with flexible backbone, i.e., variable r_{NN}: [bis(pyridine)iodine(I)] (solid line), 4-methylpyridine−iodine(I)−trifluoromethylpyridine (long-dashed line), and methylpyridine−hydrogen(I)−trifluoromethylpyridine (short-dashed line). (b) Potential curves for systems with a rigid backbone, i.e., r_{NN} kept fixed: r_{NN} = 4.30 (solid line), 4.88 (long-dashed line), and 5.50 Å (short-dashed line). The energies are given relative to the ground-state energy of the respective system (see the Supporting Information for details).

hydrogen bond analogue **1b**, which possesses a CH_3/CF_3-substituted backbone and an $[N\cdots H\cdots N]^+$ hydrogen bond (Figure 2), the hydrogen motion is predicted to follow an asymmetric double-well potential curve (Figure 1d), as shown with the short-dashed line in Figure 4a.

To achieve a three-center halogen bond complex showing a symmetric double-well potential for the halogen motion between the Lewis bases, a donor−donor distance, r_{NN}, beyond 4.880 Å has to be enforced. For such a system possessing a fully rigid backbone, the potential curves shown in red in Figure 3 and extracted in Figure 4b are obtained. At r_{NN} < 4.880 Å, the halogen motion follows a symmetric single-well potential (solid red lines in Figures 3 and 4b), which becomes shallow at r_{NN} = 4.880 Å (long-dashed red lines, Figure 4b). For r_{NN} > 4.880 Å, the halogen motion is described by a double-well potential (short-dashed red lines, Figure 4b) with a barrier that becomes wider and higher with increasing r_{NN}. Thus, to obtain a rapidly interconverting $[N\cdots I{-}N]^+ \rightleftarrows [N{-}I\cdots N]^+$ system, a backbone enforcing a nitrogen−nitrogen distance, $r_{NN,}$ not too far above 4.880 Å is necessary. In molecular systems with $r_{NN} \gg$ 4.880 Å, the interconversion of the $[N\cdots I{-}N]^+ \rightleftarrows [N{-}I\cdots N]^+$ becomes slow and its overall stability decreases. As a candidate for such a dynamic system, we designed the iodonium complex **2a** of (2,2′-(9,10-dimethoxyphenanthrene-3,6-diyl)dipyridine) which latter compound has a more rigid backbone and a longer nitrogen−nitrogen distance (predicted as 6.1 Å by DFT) as compared to **1a**.

Synthesis. Complexes **1a** and **1a-*d*** were synthesized by modification of reported protocols.[25] Regioselective deuteration of **3** to **3-*d*** was accomplished by BuLi-Li-DMAE (Scheme 1),[63] followed by microwave-assisted Sonogashira coupling[64] yielding **4** (**4-*d***). Subsequent fluoride-mediated TMS-deprotection[65] provided **5** (**5-*d***), which was converted to **6** (**6-*d***) by Sonogashira coupling with 1,2-diiodibenzene for a short time, giving a mixture of mono- and dicoupled products. The latter could be separated by silica gel chromatography. Another microwave-assisted Sonogashira coupling followed by TMS-deprotection provided **8** (**8-*d***). It should be emphasized that all traces of residual Cu(I) used in the Sonogashira coupling must be removed using EDTA to avoid in situ Glaser coupling occurring simultaneously to the TMS deprotection upon liberation of **8** (**8-*d***). Aqueous extraction and 2-fold purification by silica gel chromatography were, in our hands, insufficient to avoid this side reaction. Compound **8** (**8-*d***) was converted to **9** (**9-*d***) via Sonogashira coupling with 2-chloro-4-trifluoromethylpyridine. This bidentate ligand was converted to its silver tetrafluoroborate complex, which upon addition of I_2 afforded the target compound **1a** (**1a-*d***). This compound is stable in dichloromethane solution at room temperature. Following a literature protocol,[25] the analogous hydrogen bonded $[N{-}H\cdots N]^+$ complex (**1b**), here used as a reference for a comparable system in dynamic exchange, was generated by the addition of one equivalent trifluoroacetic acid to **9** (**9-*d***). An alternative synthetic route through 2-((2-ethynylphenyl)ethynyl)-4-(trifluoromethyl)pyridine, an analog of **8** that could have provided a common precursor for **9** and **9-*d***, has been evaluated but was dismissed due to decomposition in the Sonogashira coupling with 2-chloro-4-methylpyridine.

Complex **2a** was synthesized from commercially available **10** using the synthetic route shown in Scheme 2. $(CH_3O)_2SO_2$-mediated methylation followed by Negishi coupling with 2-pyridylzinc bromide furnished the bidentate ligand **12**, which was converted to the Ag(I) complex **13** by addition of $AgBF_4$ to its CD_3CN solution. Compound **2a** was prepared by addition of I_2 to the above-mentioned solution in an NMR tube at −40 °C, followed by centrifugation at low temperature to separate the silver iodide precipitate. As **2a** decomposes above −40 °C (to its protonated form), its solution was kept at low temperature throughout its NMR investigation.

Solution Structure of 1a. The formation of an $[N\cdots I\cdots N]^+$ halogen bond in **1a** was indicated by ^{15}N NMR coordination shifts, $\Delta\delta^{15}N_{coord}$s (Table 1), of comparable magnitude to those reported for related halogen bonded systems.[22,25,27,29,31] The $\Delta\delta^{15}N_{coord}$ of the nitrogens of **1a** are ∼10 ppm larger versus smaller as compared to the systems possessing two CH_3 or two CF_3 groups on their pyridine rings, respectively. This suggests that the $\delta^{15}N$ of the nitrogens of **1a** differ not only on account of their different electron densities but also due to the formation of N−I bonds of different strength and length. The observed $\Delta\delta^{15}N_{coord}$s indicate that the I^+ is closer to the more electron-rich nitrogen of the 4-CH_3 substituted pyridine ring as compared to that of the less electron-rich, 4-CF_3 substituted pyridine. These experimental findings are corroborated by theoretically predicted ^{15}N NMR chemical shifts (Table 1). Whereas the chemical shifts of the ligands are predicted with high, ∼5 ppm, accuracy, those predicted for the complexes are all 31−37 ppm too negative. Consequently, even though the calculated $\Delta\delta$ values are about 35 ppm too positive, which is not unexpected as the accurate prediction of ^{15}N NMR chemical shifts remains a challenge,[66]

DOI: 10.1021/jacs.8b09467
J. Am. Chem. Soc. 2018, 140, 13503−13513

Scheme 1. General Synthetic Route of [(4-Methyl-2-((2-((4-(trifluoromethyl)pyridin-2-yl)ethynyl)phenyl)ethynyl)pyridine)iodine]$^+$ BF_4^- (1a) and Its Deuterated Analog 1a-*d*[a]

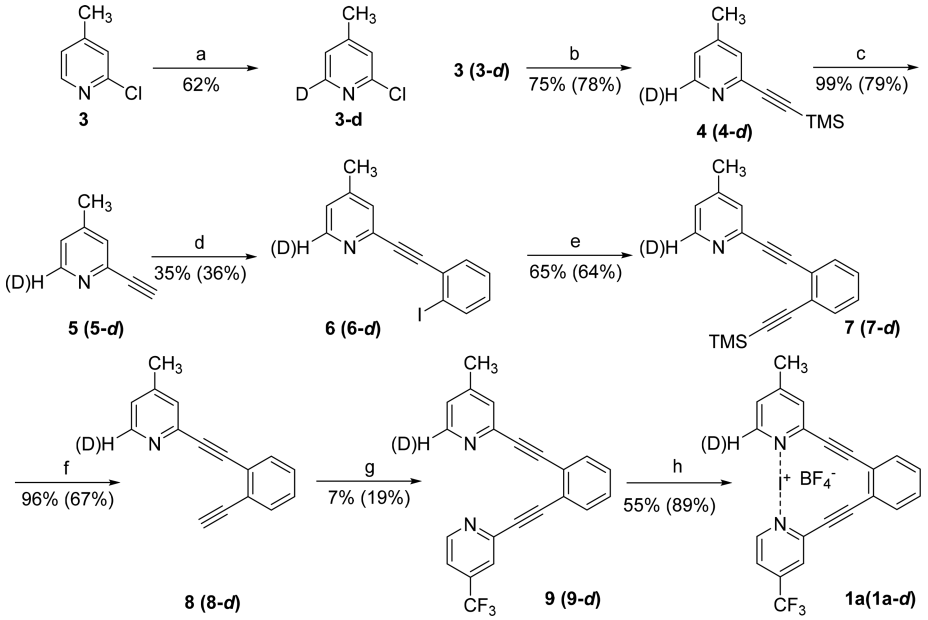

[a]Reagents and conditions: (a) 1. DMAE, *n*-BuLi, dry hexane, −78 °C, N_2; 2. MeOD, −78 °C, 30 min, −78−25 °C in 35 min; (b) TMS-acetylene, $PdCl_2(PPh_3)_2$, CuI, PPh_3, Et_2NH, MW 120 °C, 27 min; (c) MeOH, rt, 2.5 h; (d) 1,2-diiodobenzene, $Pd(PPh_3)_2Cl_2$, CuI, Et_2NH, MW 120 °C, 5 min; (e) $Pd(PPh_3)_2Cl_2$, CuI, Et_2NH, MW 120 °C, 30 min; (f) KF, MeOH, rt, 2.5 h; (g) $PdCl_2(PPh_3)_2$, CuI, Et_2NH, MW 100 °C, 12 min; (h) 1. $AgBF_4$, CH_2Cl_2, rt, 15 min; 2. I_2, CH_2Cl_2, rt, 30 min.

Scheme 2. General Synthetic Route to [(2,2′-(9,10-Dimethoxyphenanthrene-3,6-diyl)dipyridine)iodine(I)] tetrafluoroborate (2a)[a]

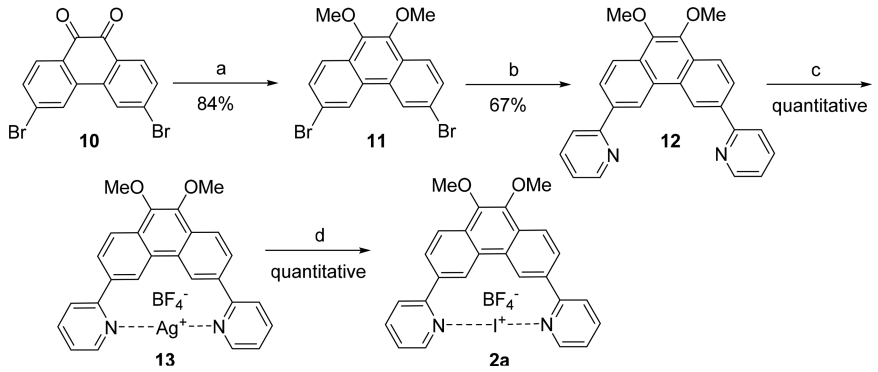

[a]Reagents and conditions: (a) Bu_4NBr, $Na_2S_2O_4$, dimethyl sulfate, THF/H_2O, 20 min; (b) $Pd(PPh_3)_4$, 2-pyridylzinc bromide, THF, 50 °C, overnight; (c) $AgBF_4$, CH_2Cl_2, 10 min; (d) I_2, CD_3CN, −40 °C.

the trends in the calculated chemical shifts are in agreement with the experimental observations.

All NMR signals of **1a** are sharp. This suggests that **1a** has either a single static geometry or is present in solution as a rapidly interconverting dynamic mixture of isomers.[23,25] To differentiate between these structural alternatives, we applied the isotopic perturbation of equilibrium (IPE) NMR technique,[67,68] which can distinguish rapidly equilibrating mixtures from static structures.[22,25,28,29,59,60,67] IPE detects vibrational energy changes upon selective isotope labeling, usually a hydrogen-to-deuterium substitution, close to the molecular site to be studied. For a mixture of isotopologues, two sets of NMR signals are observed. One set belongs to the nondeuterated compound and the other to its deuterated analog. The chemical shift difference between their signals is the isotope effect, $^n\Delta_{obs}$. It is the sum of the intrinsic isotope shift, $^n\Delta_0$, and the equilibrium isotope shift, $^n\Delta_{eq}$,[13,67] where *n* denotes the number of bonds between the detected nucleus and the position of the isotopic substitution. The intrinsic isotope effect is present in all isotopically substituted molecular systems and is typically small, attenuating as *n* increases. In contrast, the equilibrium isotope effect manifests only for dynamic molecular systems. Its magnitude is dependent on the equilibrium constant of the exchange process. Accordingly, it is zero for static molecular systems. The equilibrium isotope effect, $^n\Delta_{eq}$, is temperature dependent, as is the equilibrium constant, according to the van't Hoff equation.[69] The magnitude of the observed isotope effect, $^n\Delta_{obs}$, does not allow differentiation between a static $[N\cdots I\cdots N]^+$ and a dynamic $[N{-}I\cdots N]^+ \rightleftarrows [N\cdots I{-}N]^+$ system, but its temperature dependence does.[25]

DOI: 10.1021/jacs.8b09467
J. Am. Chem. Soc. 2018, 140, 13503−13513

Table 1. ^{15}N Chemical Shift (ppm) of the I^+ Complex 1, Its Structurally Closely Related Analogs, and the Corresponding Nitrogen Bases[a]

structure	R/R'	$\delta^{15}N_{compl}$	$\delta^{15}N_{lig}$	$\Delta\delta^{15}N_{coord}$
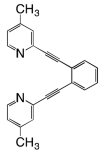	CH_3/CH_3[a]	-170.3 *-138.6*	-69.2 *-70.4*	-101.1 *-68.2*
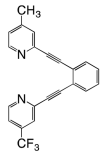	CH_3	-183.1 *-147.4*	-71.8 *-71.1*	-111.3 *-76.4*
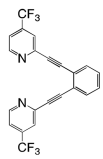	CF_3	-145.1 *-115.4*	-53.7 *-50.6*	-91.4 *-64.8*
	CF_3/CF_3[a]	-156.7 *-123.5*	-53.4 *-50.6*	-103.3 *-72.9*

[a]The ^{15}N NMR chemical shifts of the reference compounds we have previously reported.[29] Values in italic type are DFT (M06) predictions; see the Supporting Information for details.

Accordingly, we have studied a mixture of compound **1a** and its isotopologue **1a-*d*** in CD_2Cl_2 solution with the IPE technique using ^{13}C $\{^1H,^2H\}$ NMR detection, as described in detail earlier.[25,28,29] Similar to previous studies of halogen bonds, isotopologue mixtures of the free ligand **9** (Scheme 1) and of the analogous $[N{-}H{\cdots}N]^+$ hydrogen bonded complex **1b** (Figure 2) were used as references for the static and dynamic geometries, respectively (Table 2).[25,27,28] The overall

Table 2. Temperature Coefficients (ppm K) of the Isotope Shifts Observed for the CD_2Cl_2 Solutions of the $[N{\cdots}I{\cdots}N]^+$ Complex 1a, of the $[N{\cdots}I{\cdots}N]^+$ Complex 1b, and of the Free Bidentate Ligand 9, and the Sum of their Absolute Values, $\sum|\Delta_{obs}|$[a]

structure	C2 $^1\Delta_{obs}$	C3 $^2\Delta_{obs}$	C4 $^3\Delta_{obs}$	C5 $^4\Delta_{obs}$	C6 $^3\Delta_{obs}$	$\sum$ $\lvert\Delta_{obs}\rvert$
1a	−7.3	−9.9	+1.7	0	−3.4	22.3
9	−6.5	−6.5	+5.8	0	−5.9	24.7
1b	+6.0	−10.2	−22.7	0	−10.3	49.2

[a]All $^{13}C\{^1H,^2H\}$ NMR experiments were run at 125.71 MHz for the temperature interval −32 to 40 °C.

temperature dependence of the isotope effects, $\sum|\Delta_{obs}|$, of **1a** is comparable to that of the static reference **9** and is significantly smaller than that of the dynamic reference **1b**. This indicates that **1a** is a static complex, which is supported by the temperature dependence of its individual isotope shifts being primarily dependent on the distance of the observed nuclei from the position of ^2H-substitution. Further corroboration comes from the T_2 relaxation rate of H-2 (Figure 2), the proton closest to the pyridine nitrogen of **1a** (T_2 = 1.7 ± 0.9 s), which is a comparable value to that of the static reference **9** (T_2 = 1.4 ± 0.2 s) and is significantly slower than that of the hydrogen bonded complex **1b** (T_2 = 0.7 ± 0.6 s) involved in an $[N{-}H{\cdots}N]^+ \rightleftarrows [N{\cdots}H{-}N]^+$ dynamic exchange process.[22,25] Overall, ^{15}N NMR chemical shifts in combination with isotopic perturbation and relaxation NMR data reveal **1a** to prefer a static and asymmetric three-center halogen bond.

Our experimental findings are supported by quantum-chemical calculations [M06/mixed-level (double-ζ/triple-ζ/augmented triple-ζ) basis set; for details see the Supporting Information] for **1a**, **1b**, and their close structural analogs (Table 3). For **1a**, the asymmetric single-well energy potential

Table 3. Bond Distances (Å) and Relative Energies (kJ mol^{-1}) for 1a, 1b, and Their Analogs

structure	R	R′	state	r(NX)	r(N′X)	ΔE[b]	ΔE[c]
			X = I				
	H	H	GM	2.280	2.280	0	
	CH_3	CH_3	GM	2.278	2.278	−9.4	
	CF_3	CF_3	GM	2.282	2.282	30.0	
1a	CH_3	CF_3	GM	2.239	2.331	9.7	
			X = H				
	H	H	dGM	1.045	1.900	0	0
			TS	1.309	1.309		22.0
	CH_3	CH_3	dGM	1.043	1.900	−9.5	0
			TS	1.314	1.314		21.5
	CF_3	CF_3	dGM	1.042	1.923	27.3	0
			TS	1.312	1.312		23.7
1b	CH_3	CF_3	GM	1.039	1.937	−0.9	0
			LM	1.859	1.051		19.3
			TS	1.387	1.242		32.8

[a]GM = global minimum, LM = local minimum, d = degenerate, TS = transition state. [b]Stabilization energy relative to the corresponding compound with R = R′ = H. [c]For compounds with more than one equilibrium structure, the energy of the present structure relative to the ground-state energy.

(Figure 1c) is confirmed by the difference of 0.092 Å between its two N−I bond distances. In contrast, the analogs with two CH_3 or two CF_3 substituents show symmetric potential wells with two identical N−I bond distances each (Figure 1a) and N−I bond distances within 0.002 Å from that of the unsubstituted complex. For symmetric CH_3 substitution, the $[N{\cdots}I{\cdots}N]^+$ bond is predicted to be stabilized by 9.4 kJ mol^{-1} as compared to the unsubstituted analog of **1a**, [(1,2-bis(2-pyridylethynyl)benzene)iodine(I)],[25] whereas symmetric CF_3 substitution causes a 30.0 kJ mol^{-1} destabilization. The three-center bond of **1a** is computed to be 9.7 kJ mol^{-1} less stable than the unsubstituted reference. The stabilization energy of **1a** is roughly halfway between those of the symmetric CH_3 and CF_3 substituted complexes, which can be comprehended in the way that each of the N−I bonds in **1a** has approximately the same strength as an N−I bond in the corresponding bond distance for symmetric substituents. A combination of two N−I bonds with different strengths as in **1a** gives rise to an asymmetric $[N{-}I{\cdots}N]^+$ bond. For **1b**, however, an asymmetric double-well (Figure 1d) is found. In the ground state, the proton is shifted toward the CH_3-substituted pyridine. The second (local) minimum, where the proton is close to the CF_3-substituted pyridine, is 19.3 kJ mol^{-1} above the ground state. The transition state is shifted slightly toward the CF_3-substituted pyridine, and the barrier is 32.8 kJ mol^{-1} relative to the global minimum and thus (32.8−19.3) kJ mol^{-1} = 13.5 kJ mol^{-1} relative to the local minimum. The barrier height is in the same order of magnitude as that for the structural analogs with two equal substituents (Table 3). Thus, DFT calculations corroborate that **1a** is a static, asymmetric complex, whereas **1b**

DOI: 10.1021/jacs.8b09467
J. Am. Chem. Soc. 2018, 140, 13503−13513

exists as a mixture of rapidly interconverting isomers in solution.

Solution Structure of 2. Compound **13** was converted to **2a** (Scheme 2) under dry conditions at −40 °C in an NMR tube using CD_3CN as solvent. The tube was centrifuged at −40 °C and transferred into an NMR magnet with a precooled (−40 °C) probe. The vastly broadened ^1H NMR signals (Figure 5) observed for **2a** indicate it to be involved in a

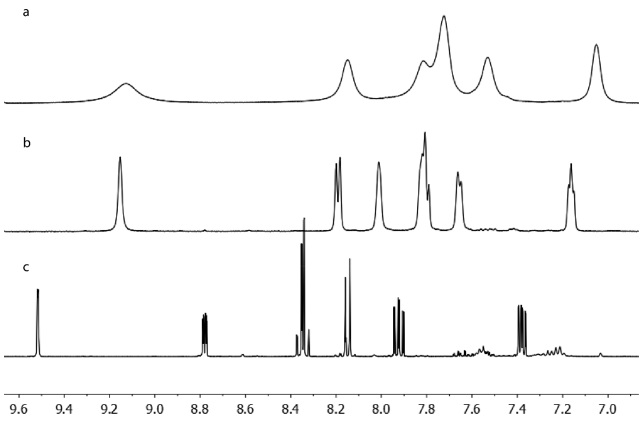

Figure 5. Aromatic region of the ^1H NMR spectrum of (a) the I^+ complex **2a**, (b) the proton complex **2b**, and (c) the free ligand **12** acquired at −40 °C for CD_3CN solution at 500 MHz suggests **2a** to be present in solution as a dynamic mixture. The signals of **2b** are also broadened but to a lesser extent than those of **2a**, suggesting a faster rate of H^+ exchange compared to that of I^+ in the corresponding halogen complex.

dynamic exchange process. This was confirmed by the rapid T_2 relaxation of the protons situated most proximately to its nitrogen donor atoms (**2a** H-2:0.0070 ± 0.0009 s; H-12:0.0030 ± 0.0005 s, **12** H-2:0.24 ± 0.16 s; H-12:0.29 ± 0.03 s; for assignments see Figure 4). The extensive line broadening prohibited the detection of ^{15}N NMR chemical shifts and the measurement of isotopic perturbation of equilibria for **2a**. The ^1H NMR signals of the analogous proton complex **2b** exhibit less extensive line broadening than **2a**. This is explained by a different rate of exchange for the dynamic processes that **2a** and **2b** undergo. Overall, NMR spectroscopy indicates **2a** to be a dynamic molecular system, with its nitrogen atoms involved in an exchange process. The specific dynamic process could not be identified by NMR.

To rationalize the experimental findings, we have computationally investigated the potential-energy landscape for **2a** and **2b** (see Scheme 3). Electronic energies and Gibbs free energies are given relative to the [bis(pyridine)iodine(I)] **14a** and the [bis(pyridine)hydrogen(I)] **14b**, respectively, as reference (i.e., as stabilization energies relative to **14a,b**). The electronic energies have been decomposed into the halogen bond energy, ΔE_{bond}, the strain energy of the backbone, ΔE_{strain}, and, where applicable, the van der Waals energy between the monomers, ΔE_{vdW} (see Table 4; details of the computations are given in the Supporting Information). The asymmetric geometry of **2a** (**2a-asy**, r_{NI} = 2.142 and 3.212 Å, r_{NN} = 5.240 Å, Scheme 3) is predicted by DFT to be a transition state (TS) between a symmetric structure (**2a-sym-1**, r_{NI} = 2.366 and 2.373 Å, r_{NN} = 4.723 Å) and one that has a covalent N−I bond while lacking an N···I halogen bond (**2a-1**, r_{NI} = 2.091 and 5.878 Å, r_{NN} = 6.468 Å). Accordingly, **2a-1** has comparable ΔE_{bond} to the reference compound **15a**, whereas **2a-asy** and **2a-sym-1** are considerably less stable, the difference in ΔG^{233} as compared to **2a-1** being 36 and 26 kJ mol^{-1}, respectively (Table 4). As reflected by the 100.3 kJ mol^{-1} (ΔE_{bond}) of **2a-asy**, its [N−I···N]$^+$ bond is considerably weaker than that of **14a**, largely because of its nonplanarity. The geometry **2a-asy** has a ΔE_{bond} 7 kJ mol^{-1} below those of **2a-1** and **15a**, i.e., the contribution of its N···I bond to the [N−I···N]$^+$ interaction is small. Owing to the bending of the phenanthrene rings of **2a-sym-1** and **2a-asy**, their strain energies are 67 and 33 kJ mol^{-1} above that of **2a-1**, respectively, which makes them less stable than **2a-1**. We note that there is another conformer with a symmetric [N···I···N]$^+$ bond, **2a-sym-2**, which is another 67 kJ mol^{-1} (ΔG^{233}) less stable as compared to **2a-sym-1** (Table 4), mainly due to the electrostatic and steric repulsion between the I atom and the H atom in positions 12 and 12′ (Figure 2), which weakens the [N···I···N]$^+$ bond. Geometry **2a-sym-2** is a transition state between conformer **2a-2**, which resembles **2a-1** both in energy and bond properties, and its mirror image.

The geometries of **2a** shown in Scheme 3 (**2a-sym-1**, **2a-asy**, and **2a-1**, for example) reflect various stages of the dissociation process of an [N···I···N]$^+$ bond, as it is depicted by the bold black line in the right border plane of Figure 3 for the [N···I···N]$^+$ bond of the analogous [bis(pyridine)-iodine(I)] model system. At the same time, they demonstrate different ways how stable complex structures can be formed in the interplay between bond stability and backbone strain. Close to the equilibrium distance, r_{NN} = 4.511 Å, the dissociation curve of the model complex shows a relatively narrow minimum of ca. 110 kJ mol^{-1} (Figure 3) belonging to a symmetric [N···I···N]$^+$ geometry. Consequently, in this region the resulting r_{NN} value for the complex is only weakly influenced by the strain from the backbone, and ligands with quite different properties can form complexes with r_{NN} values in this range, such as, e.g., **2a-sym-1** (r_{NN} = 4.723 Å). Conversely, at r_{NN} > 5 Å the asymmetric [N−I···N]$^+$ bond geometry is more stable than the symmetric alternative at the same r_{NN} distance (short dashed red line in Figure 3). The asymmetric [N−I···N]$^+$ interaction at r_{NN} > 5 Å is considerably weaker than the [N···I···N]$^+$ bond at optimal r_{NN} 4.511 Å; however, it is more stable than the alternative symmetric [N···I···N]$^+$ bond at the same r_{NN} > 5 Å distance. Moreover, its energy depends only weakly on r_{NN}, i.e., the [N−I···N]$^+$ bond is easy to stretch. Thus, the resulting r_{NN} of the complex is determined mainly by the overall geometry and rigidity of the backbone holding the two Lewis basic sites. Thus, the r_{NN} value in **2a-1** (6.468 Å) is close to that in the free ligand **12** (6.100 Å), actually, r_{NN} is slightly longer in **2a-1** than in **12** because of electrostatic and steric repulsions between the iodonium and the H atom in position 12. The intermediate geometry **2a-asy** (r_{NN} = 5.240 Å) is favored neither by a strong [N···I···N]$^+$ bond nor by a low backbone strain and is thus the TS between **2a-sym-1** and **2a-1**.

Compound **2a** possesses a longer than optimal r_{NN} in combination with a comparably rigid backbone, which explains the low stability of the **2a-asy** geometry. The most stable arrangements of **2a** are predicted by DFT to be the dimers $(\mathbf{2a})_2$**-par** and $(\mathbf{2a})_2$**-tw**. The pyridine rings of these complexes are rotated out of the plane of the phenanthrenes with two sets of [N···I···N]$^+$ bonds formed between the two **2a** units. These are oriented in a parallel or twisted fashion, respectively. The [N···I···N]$^+$ bonds of these dimers have similar geometries to those in **14a** and their backbones have low strain energies. Accordingly, $(\mathbf{2a})_2$**-par** is 52 kJ mol^{-1} and $(\mathbf{2a})_2$**-tw** is 37 kJ mol^{-1} lower in ΔG^{233} as compared to **2a-1**, with energies being

DOI: 10.1021/jacs.8b09467
J. Am. Chem. Soc. 2018, 140, 13503−13513

Scheme 3. Calculated Electronic Energies, (ΔE, kJ mol^{-1}), Gibbs Free Energies (ΔG^{233}, kJ mol^{-1}), and Bond Distances (r_{NN} and r_{NI}, Å) for a Variety of Possible Geometries of 2a and 2b[a]

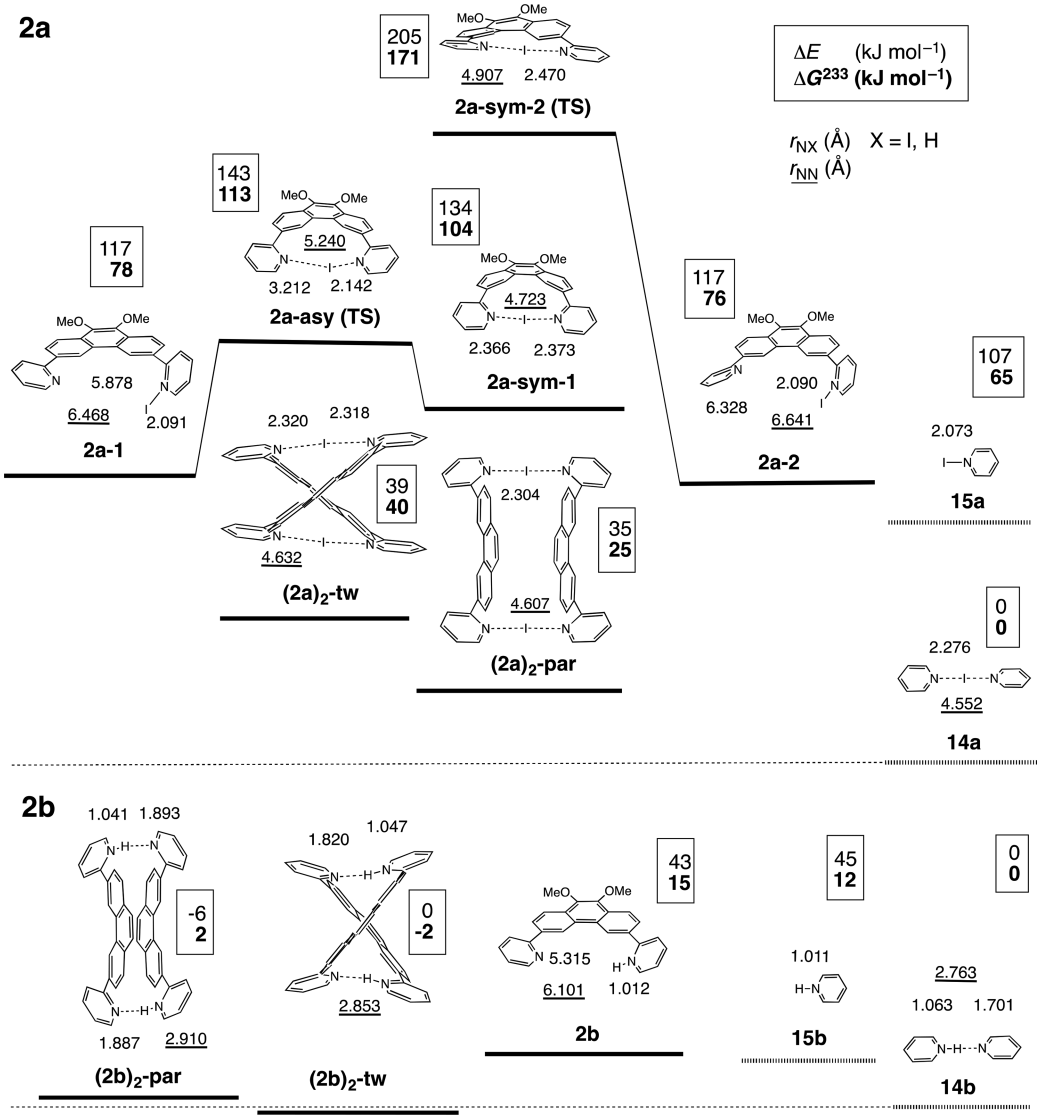

[a]Energies are given as stabilization energies relative to **14a** or **14b**, respectively; that is, positive energy values indicate that the respective compound is less stable than **14a** or **14b**, respectively. For dimeric structures, energies are given per monomer. All species shown have a charge of +2 (dimers) or +1 (others). For the dimer structures, the methoxy functionalities have been omitted to make the presentation of the bonding situation for these structures less crowded. Computational details are given in the Supporting Information.

given per monomer. Consequently, **2a** is expected to exist predominantly as **(2a)$_2$-par** and, in a second instance, as **(2a)$_2$-tw.** The most stable conformer, **(2a)$_2$-par**, remains 25 kJ mol^{-1} less stable than **14a**, suggesting **2a** to be rather unstable. This is in excellent agreement with the experimentally observed low stability of **2a**, which we could only study experimentally at −40 °C. Rapid interconversion of the **(2a)$_2$-par** and **(2a)$_2$-tw** geometries explains the NMR observed line broadening. Formation of larger oligomers, i.e., trimers or tetramers, is entropically disfavored and was therefore not studied here.

The analogous hydrogen bonded complex **2b** is predicted to also prefer forming dimeric complexes (Scheme 3b), each encompassing two asymmetric [N−H···N]$^+$ bonds with N−H bond lengths of 1.041 and 1.887 Å/1.893 Å (**(2b)$_2$-par**) and 1.047 and 1.820 Å (**(2b)$_2$-tw**), respectively. In contrast to **2a**, the twisted [**(2b)$_2$-tw**] geometry possessing a shorter N−N distance (2.853 Å versus 2.904 Å) has lower ΔG^{233}, with a difference of just 4 kJ mol^{-1} between the dimers. The dimers of **2b**, in contrast to **2a**, are further stabilized by van der Waals interaction between the two ligands, with ΔE_{vdW} values of −26 and −16 kJ mol^{-1}, respectively. The computed Gibbs free energy of these complexes is comparable to that of the analogous [bis(pyridine)hydrogen(I)] complex **14b**. This is in agreement with the experimentally detected stability of **2b** at room temperature. The observation of a single set of NMR signals suggests a rapid tautomeric exchange, [N···H−N]$^+$ ⇄ [N−H···N]$^+$, within the hydrogen bonded complexes of **2b**, which is in agreement with the previous literature.[59,60] Further details of the computational investigation are given in the Supporting Information.

CONCLUSIONS

By asymmetric alteration of the electron density of the Lewis basic nitrogens within a three-center halogen bond, a static and

DOI: 10.1021/jacs.8b09467
J. Am. Chem. Soc. 2018, 140, 13503−13513

Table 4. Stabilization Energies (kJ mol^{-1}) and Their Components for Different Conformers of 2a,b[a]

compound	ΔE_{bond}	ΔE_{strain}	ΔE_{vdW}	ΔE	ΔG^{233}
2a-1	107.6	9.8		117.3	77.6
2a-2	107.4	9.7		117.1	76.5
15a	107.3	0.0		107.3	64.7
2a-sym-1	57.2	76.7		133.8	103.8
2a-asy (TS)	100.3	42.4		142.7	113.3
2a-sym-2 (TS)	136.5	68.0		204.6	171.1
$(\mathbf{2a})_2$**-par**	14.6	18.5	2.0	35.1	25.2
$(\mathbf{2a})_2$**-tw**	28.5	14.7	−4.5	38.7	40.2
2b	43.1	−0.1		43.0	15.0
15b	44.6	0.0		44.6	11.9
$(\mathbf{2b})_2$**-par**	14.6	5.2	−25.7	−5.8	2.2
$(\mathbf{2b})_2$**-tw**	12.6	4.1	−16.3	0.4	−1.8

[a]Stabilization energies given with respect to the $[N{-}X{-}N]^+$ bond in **14a** or **14b**, respectively. For dimers, the values are given per monomer. See the Supporting Information for computational details.

asymmetric solution geometry is obtained. The halogen atom in this complex is positioned closer to the more electron-rich nitrogen, and the system is best described by an asymmetric single-well energy potential. The complex is slightly destabilized compared to its symmetric and unsubstituted analog, yet remains stable in solution at room temperature. The behavior of the halogen bond is distinctly different from that of the hydrogen bond in the analogous proton complex **1b**; the latter exists as a dynamic mixture of asymmetric geometries, $[N{\cdots}H{-}N]^+ \rightleftarrows [N{-}H{\cdots}N]^+$, with an asymmetric double-well energy potential describing the motion of H^+. This finding is consistent with the previously reported asymmetry of hydrogen bonds in solution,[59,60] as well as the distinctly different behavior of three-center halogen and hydrogen bonds.[22,23,29]

Increasing the distance between the Lewis basic sites of a bidentate ligand did not convert a static and symmetric three-center halogen bond complex into a dynamic mixture of asymmetric complexes. Complex **2a**, which has a purposely elongated N−N distance, prefers to avoid strain and forms dimers encompassing two unstrained, symmetric three-center $[N{\cdots}I{\cdots}N]^+$ halogen bonds, instead of one strained asymmetric $[N{\cdots}I{-}N]^+$ bond. The dimers interconvert between different 3D geometries, are unstable, and are therefore experimentally detectable only at low temperature. The analogous hydrogen bond complex **2b** is stable in solution at room temperature and exists as a rapidly interconverting mixture of dimers encompassing asymmetric $[N{\cdots}H{-}N]^+$ hydrogen bonds.

The three-center halogen bond, $[D{\cdots}X{\cdots}D]^+$, is extraordinarily strong, and although it can be desymmetrized, its conversion into an asymmetric $[D{-}X{\cdots}D]^+$ geometry with a distinct covalent and a distinct secondary bond is highly challenging. The difference between its behavior and that of the analogous $[D{-}H{\cdots}D]^+$ hydrogen bond may be explained by the involvement of two directional lobes of an electrophilic p-orbital on X^+ with the Lewis bases, as compared to the smaller and less directional s-orbital on H^+.

In a wider context, the current work raises the question of whether a distinction between halogen bonded systems possessing a "classical halogen bond" and those encompassing a "three-center four-electron halogen bond" is useful, or even possible, as both types of complexes involve three atomic centers that are connected by four electrons. A classical halogen bond is formed by the interaction of a Lewis base, D, with a covalently bound halogen, D−X···D, through a σ-hole, and the resulting complex encompasses a conventional two-center covalent, D−X, and a classical two-center two-electron halogen bond, D···X. Even if the formation of the halogen bond results in some lengthening and weakening of the D−X covalent bond and in the shortening of the D···X distance below the sum of the van der Waals radii of the D and X atoms, the two bonds clearly remain different. In contrast, the halogen of a three-center halogen bond is not clearly covalently or weakly bonded to either of the Lewis bases but is strongly attracted to both, with its both D···X bonds simultaneously showing covalent and secondary characters. The latter complexes have D−X bond distances (here, r(N′I) = ∼2.3 Å) in between the sum of the van der Waals radii (r_wI + r_wN = 3.5 Å) and the sum of the covalent radii (r_cI + r_cN = 2.1 Å) of the participating atoms with the halogen being roughly centered, with <10% difference between the D−X distances. Both classical and three-center bonds have covalent and electrostatic contributions, with the covalent character originating from charge transfer and the electrostatic resulting from Coulomb attraction and polarization. Dispersion has a smaller contribution, especially for strong interactions. With the decrease of halogen size, the partial covalent character of the three-center covalent bond increases[25,26] whereas the halogen bond strength, which is dominated by the electrostatic contribution, decreases. Thus, despite a larger covalent contribution and a larger reduction ratio[23,30] of an N···Cl···N bond (0.61) as compared to the analogous N···Br···N (0.63) and N···I···N (0.65) bonds, the chlorine-centered halogen bond remains the weakest and the iodine-centered bond the strongest. Accordingly, if bond strength is chosen to be characterized by binding energy, the three-center halogen bonds follow the same hierarchy as classical halogen bond interactions. However, three-center four electron halogen bonds are characteristically stronger (100−150 kJ mol^{-1})[26,29,31] than the classical halogen bonds (typically <50 kJ mol^{-1}),[70] and accordingly their formation is associated with considerably larger spectroscopic changes (i.e., $\Delta\delta^{15}N_{coord} \approx$ 100 ppm[22,23,26,29,31,58] versus <20 ppm[71]). The experimental investigations have been complemented by theoretical studies. For instance, Cremer and co-workers[72] have investigated the character of halogen bonds based on the bond strength order (BSO), a measure for the strength of individual bonds in a compound derived from its calculated vibration spectrum. If, for a $[D_1{-}X{-}D_2]$ moiety (D_1 and D_2 are the Lewis bases interacting with the halogen X), the BSO values for $[D_1{-}X]$ and $[X{-}D_2]$ are equal or nearly equal, the bond has a distinct three-center four-electron character, whereas substantially different BSO values for the two bonds indicate a classical halogen bond.

The studied model systems provide valuable insights into the fundamentals of chemical bonding and will be of significance for an improved understanding of the halogen transfer process between two halogen bond acceptors as well as the three-center-four-electron bond, whose nature and behavior remain unresolved enigmas.[54] The global energy minimum in the bonding situation of **1a** resembles the transition states of S_N2 and halonium transfer reactions.[53] We thus expect our results to provide valuable insights for the development of future halonium transfer agents.[39,40,50]

DOI: 10.1021/jacs.8b09467
J. Am. Chem. Soc. 2018, 140, 13503−13513

■ ASSOCIATED CONTENT

Supporting Information

The Supporting Information is available free of charge on the ACS Publications website at DOI: 10.1021/jacs.8b09467.

NMR and computational data and detailed information on the synthesis (PDF)

■ AUTHOR INFORMATION

Corresponding Author

*mate.erdelyi@kemi.uu.se

ORCID

Máté Erdélyi: 0000-0003-0359-5970

Present Address

‖Concept Life Sciences, Discovery Park, Ramsgate Road, Sandwich, Kent CT13 9ND, United Kingdom.

Notes

The authors declare no competing financial interest.

■ ACKNOWLEDGMENTS

We thank Martin Uhrbom, Stefan Niebling, and Daniel Sarabi (University of Gothenburg) for their contributions to the computational work in the initial phase of this project. The research leading to these results has received funding from the European Research Council under the European Union's Seventh Framework Programme (FP7/2007-2013)/ERC Grant Agreement No. 259638. We thank the Swedish Research Council (2016-03602) for financial support. This study made use of the NMR Uppsala infrastructure, which is funded by the Department of Chemistry - BMC and the Disciplinary Domain of Medicine and Pharmacy.

■ REFERENCES

(1) Desiraju, G. R.; Ho, P. S.; Kloo, L.; Legon, A. C.; Marquardt, R.; Metrangolo, P.; Politzer, P.; Resnati, G.; Rissanen, K. Definition of the Halogen Bond (Iupac Recommendations 2013). *Pure Appl. Chem.* **2013**, *85*, 1711.

(2) Cavallo, G.; Metrangolo, P.; Milani, R.; Pilati, T.; Priimagi, A.; Resnati, G.; Terraneo, G. The Halogen Bond. *Chem. Rev.* **2016**, *116*, 2478.

(3) Bondi, A. Van Der Waals Volumes and Radii. *J. Phys. Chem.* **1964**, *68*, 441.

(4) Collin, J. J. Sur L'iodide. *Ann. Chem.* **1814**, *91*, 251.

(5) Guthrie, E. XXVIII.—on the Iodide of Iodammonium. *J. Chem. Soc.* **1863**, *16*, 239.

(6) Erdelyi, M. A Big Hello to Halogen Bonding. *Nat. Chem.* **2014**, *6*, 762.

(7) Clark, T.; Hennemann, M.; Murray, J. S.; Politzer, P. Halogen Bonding: The Sigma-Hole. *J. Mol. Model.* **2007**, *13*, 291.

(8) Wang, C. W.; Danovich, D.; Mo, Y. R.; Shaik, S. On the Nature of the Halogen Bond. *J. Chem. Theory Comput.* **2014**, *10*, 3726.

(9) Mukherjee, A.; Tothadi, S.; Desiraju, G. R. Halogen Bonds in Crystal Engineering: Like Hydrogen Bonds yet Different. *Acc. Chem. Res.* **2014**, *47*, 2514.

(10) Gilday, L. C.; Robinson, S. W.; Barendt, T. A.; Langton, M. J.; Mullaney, B. R.; Beer, P. D. Halogen Bonding in Supramolecular Chemistry. *Chem. Rev.* **2015**, *115*, 7118.

(11) Ho, P. S. Biomolecular Halogen Bonds. *Top. Curr. Chem.* **2014**, *358*, 241.

(12) Wilcken, R.; Zimmermann, M. O.; Lange, A.; Joerger, A. C.; Boeckler, F. M. Principles and Applications of Halogen Bonding in Medicinal Chemistry and Chemical Biology. *J. Med. Chem.* **2013**, *56*, 1363.

(13) Erdelyi, M. Halogen Bonding in Solution. *Chem. Soc. Rev.* **2012**, *41*, 3547.

(14) Bulfield, D.; Huber, S. M. Halogen Bonding in Organic Synthesis and Organocatalysis. *Chem. - Eur. J.* **2016**, *22*, 14434.

(15) Desiraju, G. R.; Parthasarathy, R. The Nature of Halogen···Halogen Interactions - Are Short Halogen Contacts Due to Specific Attractive Forces or Due to Close Packing of Nonspherical Atoms. *J. Am. Chem. Soc.* **1989**, *111*, 8725.

(16) Hassel, O. Structural Aspects of Interatomic Charge-Transfer Bonding. *Science* **1970**, *170*, 497.

(17) Legon, A. C. Prereactive Complexes of Dihalogens XY with Lewis Bases B in the Gas Phase: A Systematic Case for the Halogen Analogue B - XY of the Hydrogen Bond B - HX. *Angew. Chem., Int. Ed.* **1999**, *38*, 2686.

(18) Bertran, J. F.; Rodriguez, M. Detection of Halogen Bond Formation by Correlation of Proton Solvent Shifts 0.1. Haloforms in Normal-Electron Donor Solvents. *Org. Magn. Reson.* **1979**, *12*, 92.

(19) Metrangolo, P.; Neukirch, H.; Pilati, T.; Resnati, G. Halogen Bonding Based Recognition Processes: A World Parallel to Hydrogen Bonding. *Acc. Chem. Res.* **2005**, *38*, 386.

(20) Metrangolo, P.; Resnati, G. Halogen Bonding: A Paradigm in Supramolecular Chemistry. *Chem. - Eur. J.* **2001**, *7*, 2511.

(21) Amico, V.; Meille, S. V.; Corradi, E.; Messina, M. T.; Resnati, G. Perfluorocarbon-Hydrocarbon Self-Assembling. 1D Infinite Chain Formation Driven by Nitrogen···Iodine Interactions. *J. Am. Chem. Soc.* **1998**, *120*, 8261.

(22) Carlsson, A.-C. C.; Gräfenstein, J.; Laurila, J. L.; Bergquist, J.; Erdélyi, M. Symmetry of $[N{-}X{-}N]^{+}$ Halogen Bonds in Solution. *Chem. Commun.* **2012**, *48*, 1458.

(23) Hakkert, S. B.; Erdelyi, M. Halogen Bond Symmetry: The N-X-N Bond. *J. Phys. Org. Chem.* **2015**, *28*, 226.

(24) Lin, G. H. Y.; Hope, H. Crystal-Structure of Bis(Thiourea)-Iodine(I) Iodide. *Acta Crystallogr., Sect. B: Struct. Crystallogr. Cryst. Chem.* **1972**, *28*, 643.

(25) Carlsson, A.-C. C.; Gräfenstein, J.; Budnjo, A.; Laurila, J. L.; Bergquist, J.; Karim, A.; Kleinmaier, R.; Brath, U.; Erdelyi, M. Symmetric Halogen Bonding Is Preferred in Solution. *J. Am. Chem. Soc.* **2012**, *134*, 5706.

(26) Karim, A.; Reitti, M.; Carlsson, A.-C. C.; Gräfenstein, J.; Erdelyi, M. The Nature of $[N\text{-}Cl\text{-}N]^{+}$ and $[N\text{-}F\text{-}N]^{+}$ Halogen Bonds in Solution. *Chem. Sci.* **2014**, *5*, 3226.

(27) Carlsson, A.-C. C.; Uhrbom, M.; Karim, A.; Brath, U.; Gräfenstein, J.; Erdelyi, M. Solvent Effects on Halogen Bond Symmetry. *CrystEngComm* **2013**, *15*, 3087.

(28) Bedin, M.; Karim, A.; Reitti, M.; Carlsson, A.-C. C.; Topic, F.; Cetina, M.; Pan, F. F.; Havel, V.; Al-Ameri, F.; Sindelar, V.; Rissanen, K.; Gräfenstein, J.; Erdelyi, M. Counterion Influence on the N-I-N Halogen Bond. *Chem. Sci.* **2015**, *6*, 3746.

(29) Carlsson, A.-C. C.; Mehmeti, K.; Uhrbom, M.; Karim, A.; Bedin, M.; Puttreddy, R.; Kleinmaier, R.; Neverov, A. A.; Nekoueishahraki, B.; Gräfenstein, J.; Erdelyi, M.; Rissanen, K. Substituent Effects on the $[N{-}I{-}N]^{+}$ Halogen Bond. *J. Am. Chem. Soc.* **2016**, *138*, 9853.

(30) Troff, R. W.; Makela, T.; Topic, F.; Valkonen, A.; Raatikainen, K.; Rissanen, K. Alternative Motifs for Halogen Bonding. *Eur. J. Org. Chem.* **2013**, *2013*, 1617.

(31) Carlsson, A.-C. C.; Veiga, A. X.; Erdélyi, M. Halogen Bonding in Solution. *Top. Curr. Chem.* **2014**, *359*, 49.

(32) Koskinen, L.; Jaaskelainen, S.; Hirva, P.; Haukka, M. Tunable Interaction Strength and Nature of the S···Br Halogen Bonds in [(Thione)Br-2] Systems. *Cryst. Growth Des.* **2015**, *15*, 1160.

(33) Koskinen, L.; Hirva, P.; Hasu, A.; Jaaskelainen, S.; Koivistoinen, J.; Pettersson, M.; Haukka, M. Modification of the Supramolecular Structure of [(Thione)IY] (Y = Cl, Br) Systems by Cooperation of Strong Halogen Bonds and Hydrogen Bonds. *CrystEngComm* **2015**, *17*, 2718.

(34) Koskinen, L.; Hirva, P.; Kalenius, E.; Jaaskelainen, S.; Rissanen, K.; Haukka, M. Halogen Bonds with Coordinative Nature: Halogen Bonding in a $S^{-}I^{+}$-S Iodonium Complex. *CrystEngComm* **2015**, *17*, 1231.

DOI: 10.1021/jacs.8b09467
J. Am. Chem. Soc. 2018, 140, 13503−13513

(35) Turunen, L.; Warzok, U.; Schalley, C. A.; Rissanen, K. Nano-Sized I12l6Molecular Capsules Based on the [N···I$^+$···N] Halogen Bond. *Chem.* **2017**, *3*, 861.
(36) Turunen, L.; Warzok, U.; Puttreddy, R.; Beyeh, N. K.; Schalley, C. A.; Rissanen, K. [NI$^+$N] Halogen-Bonded Dimeric Capsules from Tetrakis(3-Pyridyl)Ethylene Cavitands. *Angew. Chem., Int. Ed.* **2016**, *55*, 14033.
(37) Okitsu, T.; Yumitate, S.; Sato, K.; In, Y.; Wada, A. Substituent Effect of Bis(Pyridines)Iodonium Complexes as Iodinating Reagents: Control of the Iodocyclization/Oxidation Process. *Chem. - Eur. J.* **2013**, *19*, 4992.
(38) Barluenga, J. Recent Advances in Selective Organic Synthesis Mediated by Transition Metal Complexes. *Pure Appl. Chem.* **1999**, *71*, 1385.
(39) Barluenga, J.; González, J. M.; Campos, P. J.; Asensio, G. I(Py)$_2$BF$_4$, a New Reagent in Organic Synthesis: General Method for the 1, 2-Iodofunctionalization of Olefins. *Angew. Chem., Int. Ed. Engl.* **1985**, *24*, 319.
(40) Barluenga, J.; González-Bobes, F.; Murguía, M. C.; Ananthoju, S. R.; González, J. M. Bis (Pyridine) Iodonium Tetrafluoroborate (IPy$_2$BF$_4$): A Versatile Oxidizing Reagent. *Chem. - Eur. J.* **2004**, *10*, 4206.
(41) Lown, J. W.; Joshua, A. V. Electrophilic Additions of Iodonium Nitrate to Unsaturated Substrates. *Can. J. Chem.* **1977**, *55*, 122.
(42) Simonot, B.; Rousseau, G. Oxygen Effect in the Iodo Lactonization of Unsaturated Carboxylic Acids Leading to 7-to 12-Membered Ring Lactones. *J. Org. Chem.* **1994**, *59*, 5912.
(43) Brunei, Y.; Rousseau, G. Iodination of Phenols and Anilines with Bis (Sym-Collidine) Iodine (I) Hexafluorophosphate. *Tetrahedron Lett.* **1995**, *36*, 8217.
(44) Brunel, Y.; Rousseau, G. An Easy Preparation of Iodoacetylenes. *Tetrahedron Lett.* **1995**, *36*, 2619.
(45) Homsi, F.; Rousseau, G. 4-Endo-T Rig Cyclization Processes Using Bis (Collidine) Bromine (I) Hexafluorophosphate as Reagent: Preparation of 2-Oxetanones, 2-Azetidinones, and Oxetanes. *J. Org. Chem.* **1999**, *64*, 81.
(46) Rousseau, G.; Robin, S. Halogenation of Pyridinols Using Bis (Sym-Collidine) Iodine(I) and Bis(Sym-Collidine) Bromine(I) Hexafluorophosphate. *Tetrahedron Lett.* **1997**, *38*, 2467.
(47) Rousseau, G.; Robin, S. Bis(Sym-Collidine)Bromine(I) Hexafluorophosphate as Oxidant. *Tetrahedron Lett.* **2000**, *41*, 8881.
(48) Andre, V.; Lahrache, H.; Robin, S.; Rousseau, G. Reaction of Unsaturated Phosphonate Monoesters with Bromo-and Iodo (Bis-Collidine) Hexafluorophosphates. *Tetrahedron* **2007**, *63*, 10059.
(49) Neverov, A. A.; Brown, R. Mechanistic Evaluation of the Transfer of Br+ from Bis (Sym-Collidine) Bromonium Triflate to Acceptor Alkenes. *J. Org. Chem.* **1998**, *63*, 5977.
(50) Barluenga, J.; Vázquez-Villa, H.; Ballesteros, A.; Gonzàlez, J. M. Cyclization of Carbonyl Groups onto Alkynes Upon Reaction with IPy$_2$BF$_4$ and Their Trapping with Nucleophiles: A Versatile Trigger for Assembling Oxygen Heterocycles. *J. Am. Chem. Soc.* **2003**, *125*, 9028.
(51) Fujioka, H.; Nakahara, K.; Hirose, H.; Hirano, K.; Oki, T.; Kita, Y. Intramolecular Iodoetherification of Ene or Diene Ketals: Facile Synthesis of Spiroketals. *Chem. Commun.* **2011**, *47*, 1060.
(52) Aubert, E.; Espinosa, E.; Nicolas, I.; Jeannin, O.; Fourmigue, M. Toward a Reverse Hierarchy of Halogen Bonding between Bromine and Iodine. *Faraday Discuss.* **2017**, *203*, 389.
(53) Firestone, R. A. Application of Linnett Electronic Theory to Organic Chemistry.4. S_N2 Transition State. *J. Org. Chem.* **1971**, *36*, 702.
(54) Landrum, G. A.; Goldberg, N.; Hoffmann, R. Bonding in the Trihalides (X_3^-), Mixed Trihalides (X_2I^-) and Hydrogen Bihalides ($X2H^-$). The Connection between Hypervalent, Electron-Rich Three-Center, Donor-Acceptor and Strong Hydrogen Bonding. *J. Chem. Soc., Dalton Trans.* **1997**, 3605.
(55) Makhotkina, O.; Lieffrig, J.; Jeannin, O.; Fourmigue, M.; Aubert, E.; Espinosa, E. Cocrystal or Salt: Solid State-Controlled Iodine Shift in Crystalline Halogen-Bonded Systems. *Cryst. Growth Des.* **2015**, *15*, 3464.
(56) Raatikainen, K.; Rissanen, K. Interaction between Amines and N-Haloimides: A New Motif for Unprecedentedly Short Br···N and I···N Halogen Bonds. *CrystEngComm* **2011**, *13*, 6972.
(57) Puttreddy, R.; Jurcek, O.; Bhowmik, S.; Makela, T.; Rissanen, K. Very Strong N–X$^+$···O-$^-$N$^+$ Halogen Bonds. *Chem. Commun.* **2016**, *52*, 2338.
(58) Bedin, M.; Karim, A.; Reitti, M.; Carlsson, A.-C. C.; Cetina, M.; Pan, F.; Havel, V.; Al-Ameri, F.; Sindelar, V.; Rissanen, K.; Gräfenstein, J.; Erdelyi, M.; Topic, F. Counterion Influence on the Nin Halogen Bond. *Chem. Sci.* **2015**, *6*, 3746.
(59) Perrin, C. L. Are Short, Low-Barrier Hydrogen Bonds Unusually Strong? *Acc. Chem. Res.* **2010**, *43*, 1550.
(60) Perrin, C. L. Symmetry of Hydrogen Bonds in Solution. *Pure Appl. Chem.* **2009**, *81*, 571.
(61) Ebrahimi, A.; Razmazma, H.; Delarami, H. S. The Nature of Halogen Bonds in [N···X···N]$^+$ Complexes: A Theoretical Study. *Phys. Chem. Res.* **2016**, *4*, 1.
(62) Zhao, Y.; Truhlar, D. G. The M06 Suite of Density Functionals for Main Group Thermochemistry, Thermochemical Kinetics, Noncovalent Interactions, Excited States, and Transition Elements: Two New Functionals and Systematic Testing of Four M06-Class Functionals and 12 Other Functionals. *Theor. Chem. Acc.* **2008**, *120*, 215.
(63) Gros, P.; Choppin, S.; Mathieu, J.; Fort, Y. Lithiation of 2-Heterosubstituted Pyridines with Buli-Lidmae: Evidence for Regio-specificity at C-6. *J. Org. Chem.* **2002**, *67*, 234.
(64) Erdelyi, M.; Gogoll, A. Rapid Homogeneous-Phase Sonogashira Coupling Reactions Using Controlled Microwave Heating. *J. Org. Chem.* **2001**, *66*, 4165.
(65) Erdelyi, M.; Langer, V.; Karlen, A.; Gogoll, A. Insight into Beta-Hairpin Stability: A Structural and Thermodynamic Study of Diastereomeric Beta-Hairpin Mimetics. *New J. Chem.* **2002**, *26*, 834.
(66) Gregusova, A.; Perera, S. A.; Bartlett, R. J. Accuracy of Computed N-15 Nuclear Magnetic Resonance Chemical Shifts. *J. Chem. Theory Comput.* **2010**, *6*, 1228.
(67) Siehl, H. U. Isotope Effects on NMR-Spectra of Equilibrating Systems. *Adv. Phys. Org. Chem.* **1987**, *23*, 63.
(68) Saunders, M.; Telkowski, L.; Kates, M. R. Isotopic Perturbation of Degeneracy - C-13 Nuclear Magnetic-Resonance Spectra of Dimethylcyclopentyl and Dimethylnorbornyl Cations. *J. Am. Chem. Soc.* **1977**, *99*, 8070.
(69) van't Hoff, J. H. Z. Die Rolle Des Osmotischen Druckes in Der Analogie Zwischen LöSungen Und Gasen. *Z. Phys. Chem.* **1887**, *1U*, 783.
(70) Duarte, D. J. R.; Angelina, E. L.; Peruchena, N. M. On the Strength of the Halogen Bonds: Mutual Penetration, Atomic Quadrupole Moment and Laplacian Distribution of the Charge Density Analyses. *Comput. Theor. Chem.* **2012**, *998*, 164.
(71) Castro-Fernandez, S.; Lahoz, I. R.; Llamas-Saiz, A. L.; Alonso-Gomez, J. L.; Cid, M. M.; Navarro-Vazquez, A. Preparation and Characterization of a Halogen-Bonded Shape-Persistent Chiral Alleno-Acetylenic Inclusion Complex. *Org. Lett.* **2014**, *16*, 1136.
(72) Oliveira, V.; Kraka, E.; Cremer, D. The Intrinsic Strength of the Halogen Bond: Electrostatic and Covalent Contributions Described by Coupled Cluster Theory. *Phys. Chem. Chem. Phys.* **2016**, *18*, 33031.

DOI: 10.1021/jacs.8b09467
J. Am. Chem. Soc. 2018, 140, 13503−13513